

Full-scale measurements and numeric simulations of driving rain on a building

Fabien J.R. van Mook

Building Physics group (FAGO), Eindhoven University of Technology (TUE),

Postbus 513, 5600 MB Eindhoven, the Netherlands, e-mail: famo@fago.bwk.tue.nl

ABSTRACT: Results of full-scale measurements and c.f.d. simulations of driving rain on a building facade and of wind at one position at 0.5 m from the facade surface, along with reference measurements, are presented. The wind is simulated by a standard K - ϵ model, and the results are compared with measurements quantitatively and qualitatively. The applied model of driving rain takes drop trajectories and raindrop spectra into account. The simulated driving rain is compared with 10-min measurements of driving rain.

1 INTRODUCTION

Many factors determine the deterioration of building envelopes. Heat and moisture transfer, dry and wet deposition of chemical substances, design deficiency and imperfections affect the performance and durability of facades, and the costs of maintenance. To design good buildings with regard to durable envelopes, knowledge of the exposure to the local outdoor climate is primordial. One of the parameters is driving rain, defined as rain that is carried by wind and driven onto the building envelope.

A standard method for building designers to estimate driving-rain quantities (BSI 1992) is available only in the UK. There are few other tools and data available, useful for the estimation of driving rain and for laboratory tests of building materials and structures. In the last decade computational fluid dynamics (c.f.d.) became available. To our knowledge, only a single attempt has been made to compare driving-rain c.f.d. simulations with wind tunnel experiments (Hangan and Surry 1998).

Since December 1997 full-scale measurements of wind and driving rain on the west facade of the Main Building of the Eindhoven University of Technology (TUE) are carried out, along with reference measurements of wind and rain. The aim is to determine the function of driving-rain quantities as function of reference wind and rain parameters. In this paper, results of the full-scale measurements and results of c.f.d. simulations of wind and driving rain of the same situation

are presented.

2 DRIVING RAIN

The general model on driving rain used in this study, has been described in van Mook et al. (1997). Such an approach is also used in e.g. Bookermann and Wisse (1992), Choi (1993), Sankaran and Paterson (1995) and Hangan and Surry (1998). A brief summary defining the quantities and symbols used in this paper is provided here.

The horizontal rain intensity R_h [mm/s] is the rate of rain water falling through a horizontal plane during a certain period in the undisturbed wind flow, and equals to the summation of the masses of all the drops falling through that plane:

$$R_h = \int_0^{\infty} \phi_h(D) dD, \quad (1)$$

with $\phi_h(D)$ = horizontal drop mass spectrum [$\text{kg m}^{-2} \text{s}^{-1} \text{m}^{-1}$], i.e. the total mass of raindrops with diameters D [m] falling on a horizontal plane in the undisturbed wind flow.

The horizontal drop mass spectrum can be calculated from the drop number spectrum $n_h(D)$ [$\text{m}^{-3} \text{m}^{-1}$]:

$$\phi_h(D) = n_h(D) v_{fall}(D) \rho \frac{\pi}{6} D^3, \quad (2)$$

with $v_{fall}(D)$ = terminal velocity [m s^{-1}] of a drop, and ρ = density [kg m^{-3}] of water.

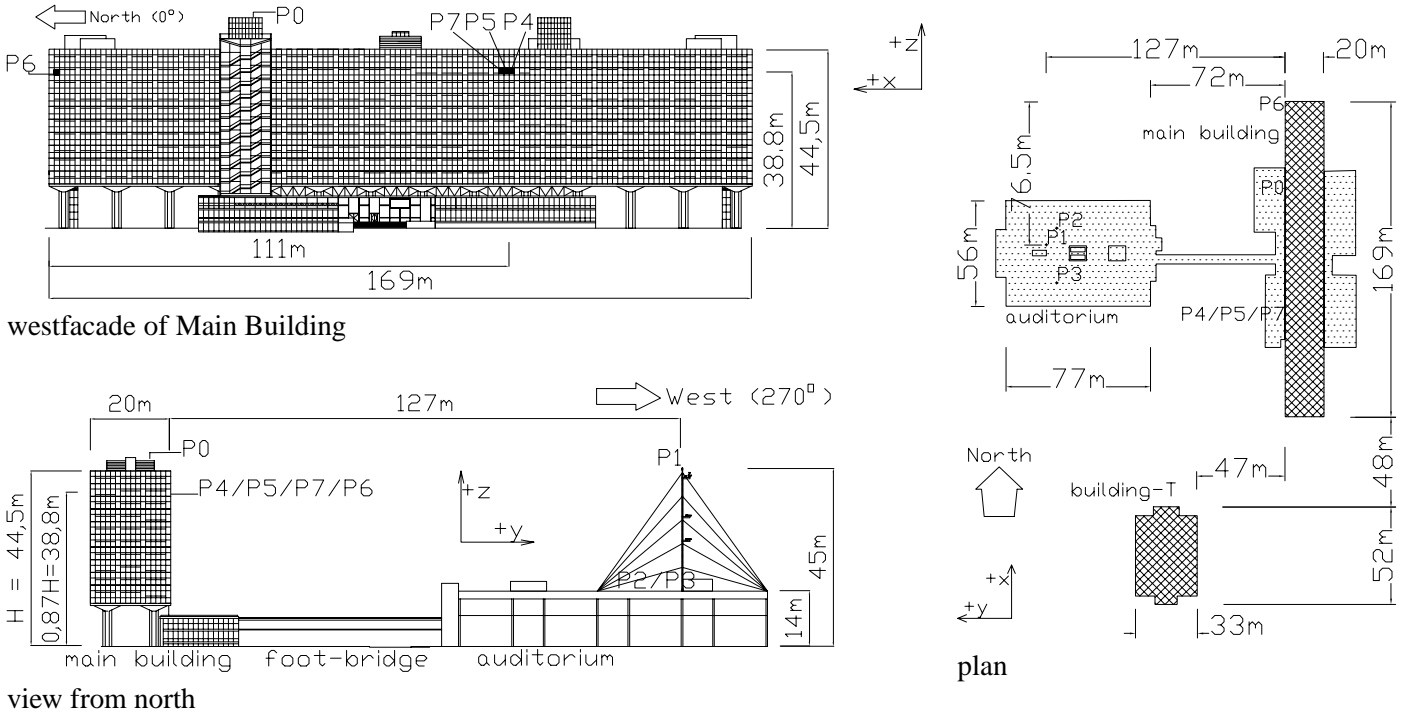


Figure 1: Test site, measurement positions P1-P7 and definition of x - y - z directions.

Before a raindrop impinges on a building facade, it has travelled from the clouds downwards, and its trajectory has been determined by the wind field, the gravitational force and drag forces. A fraction of the drops of a certain size D will impinge on a particular position on the facade:

$$\eta(D) = \frac{\phi_{dr}(D)}{\phi_h(D)}, \quad (3)$$

with $\eta(D)$ = catch ratio [-] per drop size, $\phi_{dr}(D)$ = drop mass spectrum [$\text{kg m}^{-2} \text{s}^{-1} \text{m}^{-1}$], impinging on the building envelope.

Thus, the actual driving-rain intensity R_{dr} on the building is:

$$R_{dr} = \int_0^{\infty} \eta(D) \phi_h(D) dD. \quad (4)$$

Unfortunately, one can not measure the drop mass spectrum $\phi_{dr}(D)$ on the building envelope. Therefore, a driving-rain ratio k is defined as:

$$k = \frac{R_{dr}}{R_h}. \quad (5)$$

In Lacy (1965) and BS 8104 (BSI 1992) the following relationship between the driving-rain intensity and the reference wind speed U [m s^{-1}] is assumed:

$$\frac{R_{dr}}{R_h^b} = \kappa \alpha U, \quad (6)$$

with κ = obstruction factor [-] depending on building geometry, α = free driving-rain ratio [$\text{s m}^{-1} \text{mm}^{-b} \text{h}^b$], with a constant value of 0.22 (Lacy 1965), and b = a constant, which according to Lacy (1965) equals to 0.88, here we assume $b = 1$.

3 SITE AND MEASUREMENT SET-UP

Full-scale experiments have been carried out at the Main Building on the campus of the TUE. The dimensions of the Main Building are: (height) 44.5 m, (width) 167 m and (depth) 20 m. Figure 1 shows the west facade of the Main Building: driving rain is measured at two positions, P5 and P6, and wind velocity is measured near the facade at position P4.

The site is suited because the prevailing direction for wind and rain is between south and west. There are no large obstacles in south-west to west direction. The fetch in this direction is rough (roughness length of 1 ± 0.4 m, with a displacement height of 10 m (Geurts 1997)), and consists mainly of trees over a distance of 400 m. The nearest high-rise building in this direction is 500 m away. The wind characteristics of the site have been presented in Geurts (1997).

The reference wind velocity is measured at 45 m height (from ground level) on a mast, located 127 m westwards from the Main Building (figure 1, position P1). The mast is standing on the Auditorium, which is 14 m high, 77 m long and 56 m wide, and which is located at 72 m from the Main Building.

The reference horizontal rain intensity is measured by two tipping-bucket rain gauges on the roof of the Auditorium at positions P2 and P3. Since December 1998, a disdrometer (a device to measure the rain-drop spectrum) has been installed next to one of the tipping-bucket rain gauges (P3).

The two driving-rain gauges at positions P5 and P6 have been developed at the TUE. They are identical and consist mainly of (1) a teflon coated collector (a shallow plate on which raindrops impinge and are supposed to drip downwards), (2) a wiper which improves the coagulation and dripping-down of the drops on the collector, (3) a reservoir on a balance to measure the collected rain water, see figure 2. Comparison of this type of driving-rain gauge with other types has been discussed in van Mook (1998), and will be discussed in Högberg et al. (1998).

At position P4, an ultrasonic anemometer is placed on an arm, by which the distance to the facade surface can be adjusted between 0.25 and 1.25 m.

Table 1 gives an overview of the instrumentation and the applied output sample rates.

4 SIMULATION METHOD

4.1 Wind calculation method

Simulations of the wind around the Main Building have been performed by a commercially available c.f.d. package *Fluent* (version 4.4). The used model is a standard $K-\epsilon$ model (Fluent Inc. 1995). Some important features are as follows:

- Except for $C_\mu = 0.032$, the standard values of the $K-\epsilon$ model have been applied. The C_μ constant has been adapted according to the findings of Bottema (1993), who also compared his simulations favourably with wind tunnel measurements.

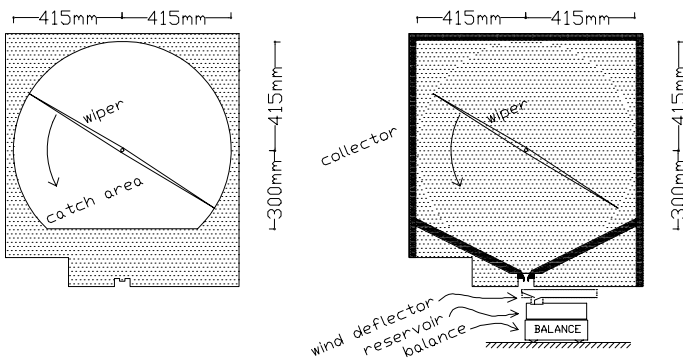


Figure 2: Driving-rain gauge, with driving-rain collector II, wind deflector, reservoir (3 litres) and balance. Left: foreplate with the round catchment area (0.492 m²). Right: backplate and the inside.

- The three-dimensional computational domain is 1190 m long in east-west direction, 1477 m long in north-south direction and 225 m high. It is divided into 95, 96 and 47 cells respectively.

Figure 3 shows the computational grid. The first grid cells on the facade of the Main Building have a thickness of 0.25 m. Care is taken to keep the grid expansion factor of two successive grid lines between 0.7 and 1.3.

The grid is a so-called structured grid, so that undesired large expansion factors and cell aspect ratios are inevitable in some parts of the grid.

- The profile of the wind coming into the domain is described by:

$$u_{<20}(z) = \frac{u_{*,1}}{0.4} \ln\left(\frac{z}{z_{0,1}}\right) \quad \text{for } z < 20\text{m}, \quad (7)$$

and:

$$u_{\geq 20}(z) = \frac{u_*}{0.4} \ln\left(\frac{z-d}{z_0}\right) \quad \text{for } z \geq 20\text{m}, \quad (8)$$

with $u(z)$ = horizontal wind velocity [m s⁻¹] at height z [m] above ground level, z_0 = roughness

Table 1: Measurement positions and instrumentation. The reference quantities (at the Auditorium) are marked with an asterisk. See also figure 1.

position	quantity/instrument [output sample rate]
P1*	wind velocity (3d) / Solent Research Ultrasonic Anemometer [1 / min]
P2*	horizontal rain intensity / Young tipping bucket rain gauge 52202 [2 / min]
P3*	horizontal rain intensity / Young tipping bucket rain gauge 52202 [2 / min]
P3*	duration of horizontal rain / home-made rain indicator [2 / min]
P3*	horizontal raindrop spectrum / Parsivel M300 (IMK Karlsruhe) [2 / min]
P4	wind velocity (3d) at 50–125 cm from facade surface / Solent Windmaster 1086M Ultrasonic Anemometer [1 / s]
P5	driving-rain intensity / driving-rain collector II with wiper + balance [2 / min]
P6	driving-rain intensity / driving-rain collector II with wiper + balance [2 / min]

length [m] for $z > 20$ m, $z_{0,1}$ = roughness length [m] for $z < 20$ m, u_* = friction velocity [m s^{-1}], $u_{*,1}$ = friction velocity [m s^{-1}] yielded from $u_{<20}(20) = u_{\geq 20}(20)$, d = displacement height [m].

The values of $z_0 = 1.0$ m and $d = 10$ m have been determined by measurements on the site (Geurts 1997). The split-up of the wind profile is necessary to account for the displacement height d of 10 m; otherwise, the wind profile below 10 m height would be undetermined. Moreover, the fetch consists of a park up to a distance of 400 m from the Main Building (therefore a estimated $z_{0,1}$ of 0.1 m) and buildings west from the park with a height of ~ 20 m.

The friction velocity u_* is based on the wind speed U_{10} at Eindhoven airport (~ 5 km westward from the Main Building, with $z = 10$ m, $z_0 = 0.03$ m and $d = 0$ m) and the measured ratio $u(45)/U_{10} = 1.13$ (Geurts 1997), which is in agreement to the internal boundary layer model of Simiu and Scanlan (1986, p. 67).

- As the facade consists of a smooth glass cladding, a value of 0.0005 m is assumed for its roughness length.

4.2 Driving-rain calculation method

The calculations of the drop trajectories have also been performed by the same c.f.d. package *Fluent* (version 4.4). The trajectories were calculated after the wind flow was calculated for a chosen geometry and reference wind speed. The trajectory calculation

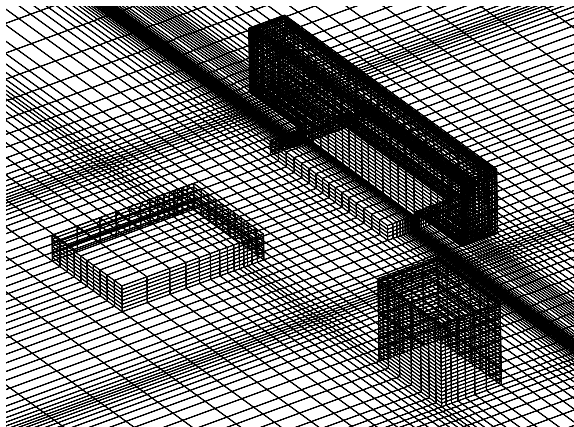


Figure 3: Computational grid. View from south-west. From left to right: the Auditorium, the Main Building and building T.

has also implications for the the computational grid: the dimensions of the grid cells in which drop trajectory deviations will occur, should be smaller than the stopping distance of the smallest drop. This implies a maximum dimension of 0.5 m near the facade, i.e. the approximate stopping distance of 1 m for a 0.5 mm drop at 2 m s^{-1} (van Mook et al. 1997). Dispersion of drops due to the turbulence of wind is not taken into account.

After the calculation of drop trajectories, catch ratios $\eta(D)$ are calculated by determining the number of drops released in the undisturbed wind field per square metre, and the number of drops impinging on a chosen position on the building facade per square metre. A total of $\sim 20,000$ drops (with $D = 0.5, 1.0, 1.5, \dots 6.0$ mm) were released in the computation domain, for every of the three chosen reference wind speeds $U_{h,ref} = 3.5, 5.7$ and 11.2 m s^{-1} , and two wind directions $\Phi_{ref} = 270^\circ$ (= normal to the facade) and $\Phi_{ref} = 300^\circ$.

5 RESULTS AND DISCUSSION

5.1 Wind

The simulations have been compared in mainly three ways:

- *Normalised wind velocities*: Figure 4a shows the wind speed at 50 cm from the facade at position P4, $U_{abs,P4}$, normalised by the horizontal wind speed $U_{h,ref}$ at position P1.

The simulated wind speeds $U_{abs,P4}$ (figure 4a) are (just) within the standard deviation of the measurements. The larger deviations are found at wind directions of $< 240^\circ$, due to the wake of building T. Building T (figures 1 and 3) has the same height as the Main Building. When building T is included in the computational domain, the results compare better with the measurements.

Figures 4b-d show the normalised velocity components at 50 cm from the facade at position P4. See figure 1 for the definition of the x - y - z axis system. The predictions made by the simulations (with inclusion of building T in the grid) of $U_{x,P4}$ are within the standard deviation of the measurements. But this does not apply for the vertical component $U_{y,P4}$, which is the second most important contribution to the wind speed at P4. In this case one should be careful interpreting the measured data: the ultrasonic anemometer at P4

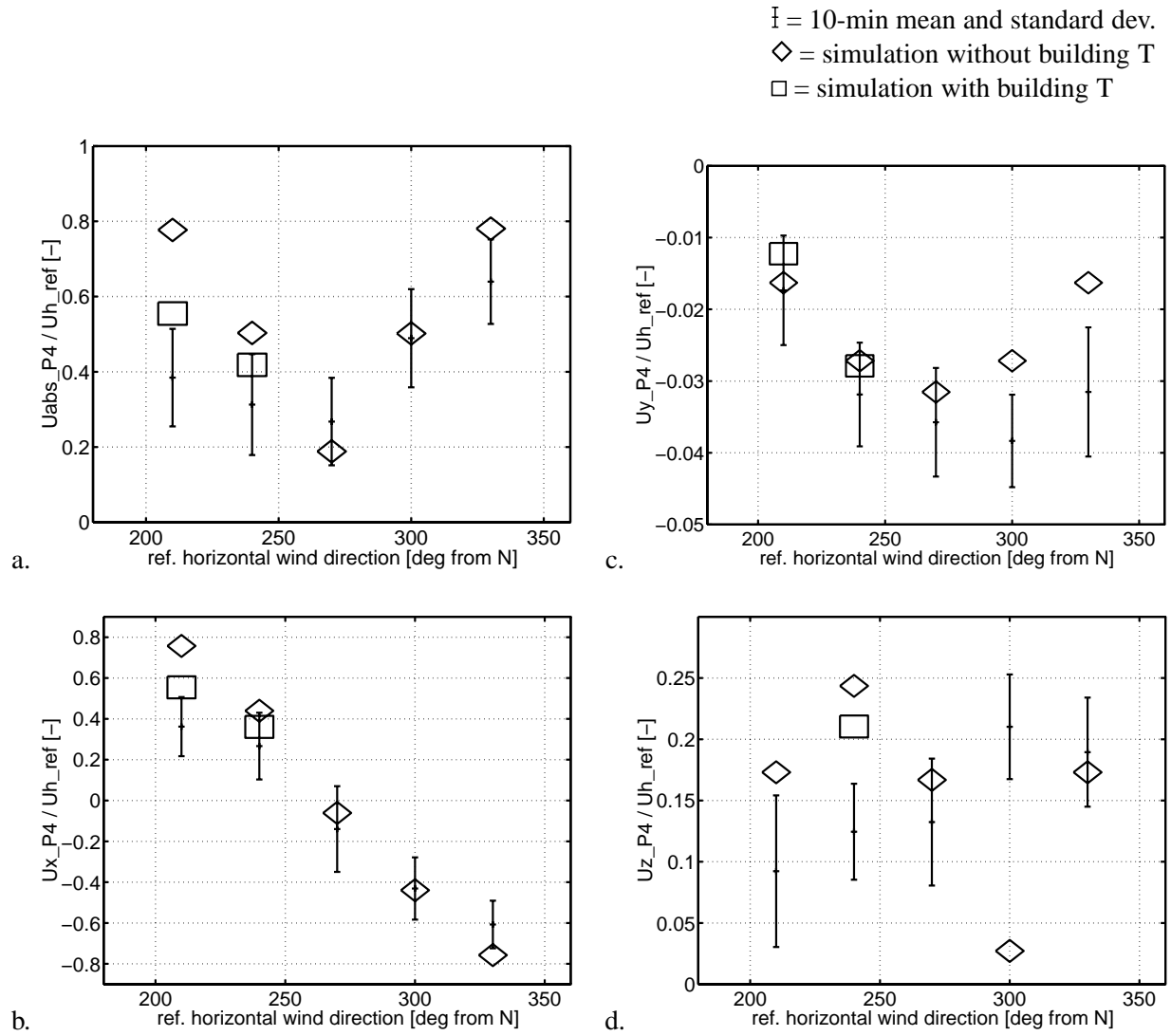


Figure 4: Measured and simulated wind velocities at 50 cm from the facade at position P4, normalised by the reference wind speed $U_{h,ref}$, as function of the reference wind direction Φ_{ref} . Figure 4a: the normalised wind speed $U_{abs,P4}$. Figure 4b-d: the normalised velocity components $U_{x,P4}$, $U_{y,P4}$ and $U_{z,P4}$.

is positioned vertically, and in this direction, the vertical wind is mostly obstructed by the housing of the anemometer.

- *Mean pressure coefficients:* Data from previous wind tunnel and full-scale measurements of mean pressure coefficients on the west facade of the Main Building (Geurts 1997) are compared with the simulation results of the current study in figure 5.

The simulated pressure coefficients at the edges show large deviations from the measurements. This might be caused by too large or non-ideally formed grid cells near the edges.

- *Qualitatively:* The simulations show recirculation on the roof and side facades.

The general difficulties of the standard $K-\epsilon$ model with the simulation of recirculation on the leeward sides and the (over-)production of turbulent kinetic energy at the windward edges of a building have been pointed out in the literature (see e.g. Murakami et al. (1992)). Literature also points out, though, that generally the wind speed values at the windward side of a building are simulated in good agreement to (wind tunnel) measurements. Seen this, the general difficulties, and the use of a structured grid with inevitably non-ideally shaped grid cells, the simulations of the present study seem to compare well enough with the measurements to proceed to the driving-rain calculations.

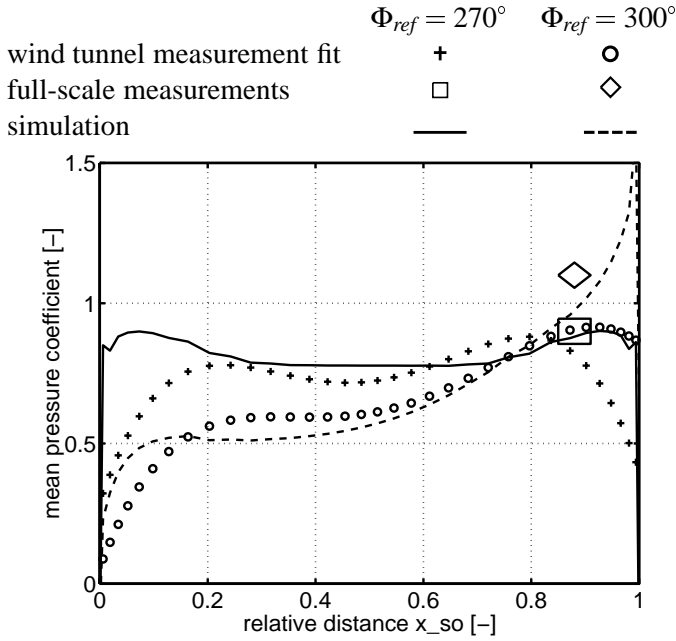


Figure 5: Measured (Geurts 1997) and simulated (current study) mean pressure coefficients as function of the position on the facade, at 72% of building height. The north edge of the west facade is represented by the relative position $x_{so} = 1$, the south edge by $x_{so} = 0$.

5.2 Driving rain

Figure 6a shows the measured driving-rain ratios k (eq. 5), at facade position P5 as function of the reference wind velocity component normal to the facade ($U_{y,ref}$), measured at P1. The 10-min values in this graph show a large scatter, although the data has been selected by the following criteria: (1) wind from west $225^\circ \leq \Phi_{ref} \leq 315^\circ$, (2) a maximum r.m.s. wind direction $\sigma_{\Phi_{ref}} < 5^\circ$, (3) a minimum for the reference horizontal rain intensity $R_h \geq 0.02$ mm/h, and, (4) a maximum relative difference in rain intensity R_h , at the two reference positions P2 and P3:

$$\frac{|R_{h,P3} - R_{h,P2}|}{R_{h,P2}} \leq 0.2.$$

By criterium 3 and 4 the relative error in R_h is limited; the other criteria have been defined to make a comparison with the simulation possible.

The measured driving-rain ratios k as function of the reference horizontal rain intensity R_h also show scatter. Figure 6b shows this for the data of figure 6a, which have been additionally selected for reference wind speeds $5 \leq U_{h,ref} \leq 7$ m s⁻¹. The driving-rain ratios do not show a clear dependency to the horizontal rain intensity. From figures 6a and 6b one can conclude that an other parameter plays a role in driving rain. Below, with the results of the driving-rain sim-

ulations, one will see that the raindrop spectrum may be this parameter.

Figure 7 gives the catch ratio $\eta(D)$ as function of facade positions P5 and P6, a reference wind direction of 240° ($= 30^\circ$ from the normal of the facade) and three reference wind speeds. The shape of the catch ratio as function of the drop diameter is as expected: smaller drops are less likely to impinge on the building facade because they are more easily carried by the wind than thicker drops. In the figure is also visible that an increase of the reference wind speed causes more drops to hit the facade. To calculate driving-rain ratios k one needs horizontal raindrop spectra $n_h(D)$. Unfortunately, usable data from the disdrometer have not yet been obtained, so raindrop spectra known from literature will be used here (Marshall and Palmer 1948), (Ulbrich 1983). See figure 8.

The resulting driving-rain ratios k , calculated from

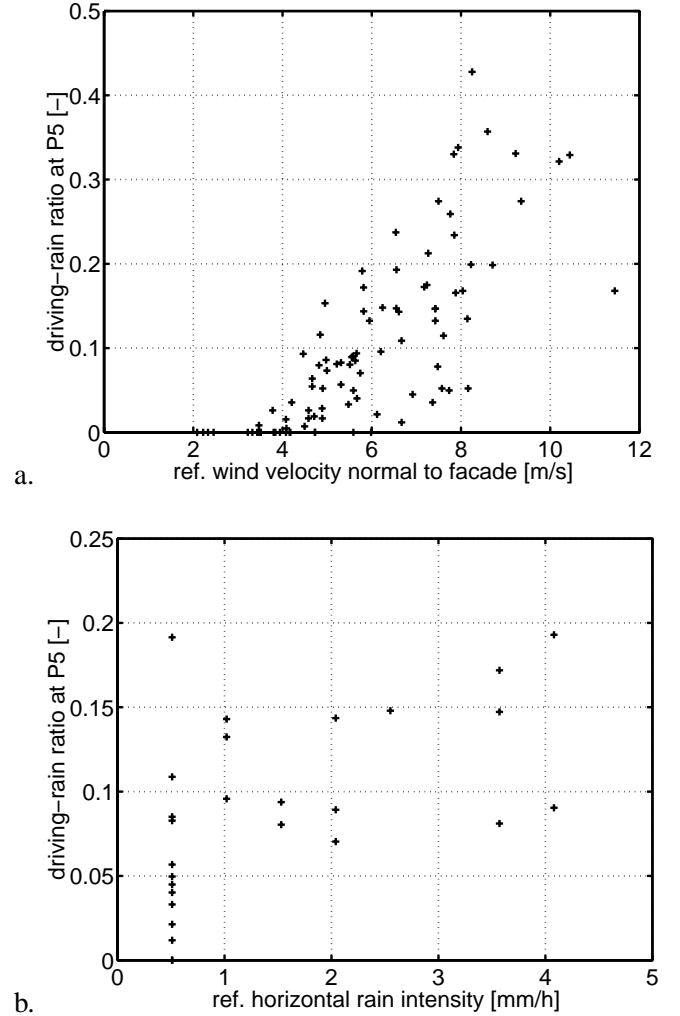


Figure 6: Measured driving-rain ratios k (10-min values) at the facade position P5, as function of (a) the reference wind velocity component normal to the facade $U_{y,ref}$ and (b) the reference horizontal rain intensity R_h .

the mentioned horizontal raindrop spectra, are shown in figure 9 with the mean and standard deviation of the measured driving-rain ratios of figure 6a. Two observations are made: Firstly, several of the simulated catch ratios for $U_{y,ref} < 6 \text{ m s}^{-1}$ are well outside of the standard deviation range of the measurements. An explanation might be that the chosen raindrop spectra are not realistic. For a reference wind speed $U_{y,ref} < 4 \text{ m s}^{-1}$, the overestimation of the simulated driving-

measurements: \bar{I} = mean and stand. dev. k
simulations : ∇ = 0.1 mm/h, \square = 1 mm/h,
 \diamond = 5 mm/h (R_h)

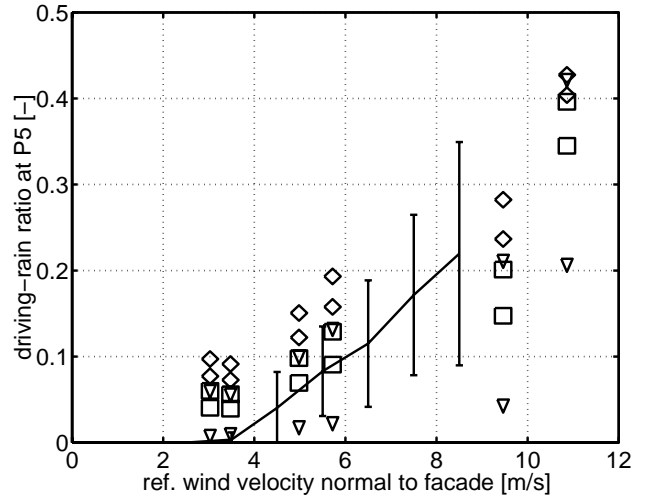


Figure 9: Measured and simulated driving-rain ratios k at the facade position P5, as function of the reference wind velocity component normal to the facade $U_{y,ref}$ and the reference horizontal rain intensity R_h . Cf. figure 6a.

rain ratio is apparent, and this may be due to not yet investigated errors in the simulation of wind velocity field and raindrop trajectories.

Secondly, the influence of the shape of the raindrop spectrum is also visible in the simulated catch ratios of figure 9: different raindrop spectra with the same rain intensity yield different catch ratios. This is an indication for the previously stated assumption that the driving-rain ratio k does not primarily depend on the horizontal rain intensity but on the raindrop spectrum.

Finally, a note is made on the relationship formulated in Lacy (1965) and BS 8104 (BSI 1992) (eq. 6) with regard to the measurements of the present study. The measured catch ratios of figure 6a can be well fitted in a linear relationship like eq. 6, provided that one should take $U_{y,ref}$ for U and account for $k = 0$ at $U_{y,ref} < \sim 2 \text{ m s}^{-1}$.

6 CONCLUSIONS

In spite of the limitations of the applied $K-\epsilon$ model and the practically limited number of grid cells of the applied structured grid, the simulated wind speed at the facade is within the standard deviation of the measurements. The simulated mean pressure coefficient at the windward facade agrees well with measurements of previous studies at the Main Building of the TUE. However, the mean pressure coefficient is overestimated at the edges of the windward facade.

	P5	P6
$U_{y,ref} = 3.1 \text{ m s}^{-1}, \Phi_{ref} = 240^\circ$	—	- - -
$U_{y,ref} = 5.0 \text{ m s}^{-1}, \Phi_{ref} = 240^\circ$	⋯	- · - ·
$U_{y,ref} = 9.5 \text{ m s}^{-1}, \Phi_{ref} = 240^\circ$	⋯+⋯	⋯○⋯

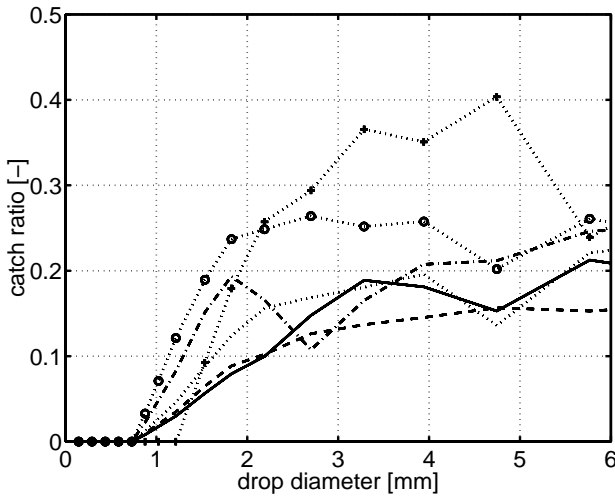


Figure 7: Simulated catch ratio $\eta(D)$ at facade positions P5 and P6 for wind direction $\Phi_{ref} = 240^\circ$.

⋯○⋯ = Marshall and Palmer
⋯+⋯ = Ulbrich

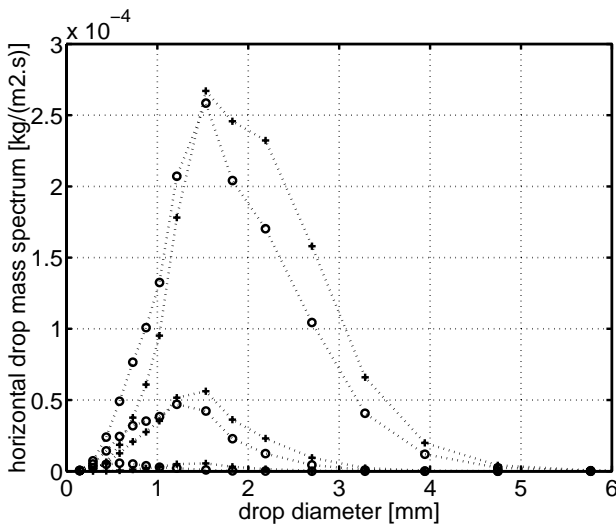


Figure 8: Horizontal drop mass spectrum $\phi_i(D)$ per drop size interval for reference horizontal rain intensities $R_h = 0.1, 1.0$ and 5.0 mm/h and two raindrop spectra.

With raindrop spectra known from literature, driving rain is simulated. Some of the simulated driving-rain ratios are well outside the standard deviation of the measured driving-rain ratio, especially at low wind speeds ($U_{y,ref} < 4 \text{ m s}^{-1}$). A further investigation should bring clarity, whether it is mainly due to errors in the calculation of the wind velocity field, the drop trajectories or the chosen raindrop spectra.

The 10-min values of the driving-rain ratio k show a large scatter, even selected for a reference wind velocity interval $U_{y,ref}$, a maximum r.m.s. wind direction $\sigma_{\Phi_{ref}}$, and a minimum horizontal rain intensity R_h . The standard deviation of k as function of $U_{y,ref}$ is $\sim 50\%$ of the mean value of k . The scatter of 10-min values of k does not only seem to depend on the mentioned parameters but is presumably also due to variations in raindrop spectra, as is also visible in the simulations. Further research will include raindrop spectrum measurements by a disdrometer to verify this.

ACKNOWLEDGEMENTS

This research is a joint project of the Faculty of Architecture, Planning and Building and of the Faculty of Technical Physics, at the TUE. The project is partly funded by the common TUE programme on ‘Technology for Sustainable Development’.

The fruitful discussions with and the suggestions of dr. Marcel Bottema, dr.ir. Chris Geurts, prof.dr.ir. Klaas Kopinga, dr. Suresh Kumar M.Sc., prof.ir. Jacob Wisse and dr.ir. Martin de Wit are greatly acknowledged.

REFERENCES

Bookermann, J. and J. Wisse (1992). Numerical estimate of driving rain. In *Inaugural Conference of the Wind Engineering Society*, 28–30 Sept., Cambridge (UK). Wind Engineering Society.

Bottema, M. (1993). *Wind climate and urban geometry*. Ph. D. thesis, Eindhoven University of Technology.

BSI (1992). *BS 8104: Code of practice for assessing exposure of walls to wind-driven rain*. BSI.

Choi, E. (1993). Simulation of wind-driven-rain around a building. *Journal of Wind Engineering and Industrial Aerodynamics* 46/47, 721–729.

Fluent Inc. (1995). *Fluent user’s guide; Version 4.3*. Fluent Inc.

Geurts, C. (1997). *Wind induced pressure fluctuations*

on building facades. Ph. D. thesis, Eindhoven University of Technology.

Hangan, H. and D. Surry (1998). Wind-driven rain on buildings: A C-FD-E approach. In *Proceedings of the 4th UK Conference on Wind Engineering, Bristol (UK)*, 2–4 September 1998, pp. 23–28. Wind Engineering Society.

Högberg, A., M. K. Kragh, and F. van Mook (1998). A comparison of driving rain measurements with different gauges. Paper accepted for *5th Symposium of Building Physics in the Nordic Countries*, Göteborg, 24–26 August 1999.

Lacy, R. (1965). Driving-rain maps and the onslaught of rain on buildings. In *RILEM/CIB Symposium on Moisture in Buildings, Helsinki (SF)*.

Marshall, J. and W. Palmer (1948). The distribution of raindrops with size. *Journal of Meteorology* 5, 165–166.

Murakami, S., A. Mochida, Y. Hayashi, and S. Sakamoto (1992). Numerical study on velocity-pressure field and wind forces for bluff bodies by k - ϵ , ASM and LES. *Journal of Wind Engineering and Industrial Aerodynamics* 41–44, 2841–2852.

Sankaran, R. and D. Paterson (1995). Computation of rain falling on a tall rectangular building. In *9th International Conference on Wind Engineering, New Delhi, India*, pp. 2127–2137. International Association for Wind Engineering.

Simiu, E. and R. Scanlan (1986). *Wind effects on structures* (2 ed.). John Wiley & Sons, New York.

Ulbrich, C. (1983). Natural variations in the analytical form of the raindrop size distribution. *Journal of Climate and Applied Meteorology* 22(10), 1764–1775.

van Mook, F. (1998). Measurements of driving rain by a driving-rain gauge with a wiper. Paper presented at *CIB taskgroup 21 meeting, Gävle (SE)*, 5/6 June.

van Mook, F., M. de Wit, and J. Wisse (1997). Computer simulation of driving rain on building envelopes. In *Proceedings of the 2nd European and African Conference on Wind Engineering*, 22–26 June 1997, Genova (IT), pp. 1059–1066.